Measurement of hadron and lepton-pair production from e^+e^- annihilation at centre-of-mass energies of 130 and 136 GeV

D. Buskulic, I. de Bonis, D. Decamp, P. Ghez, C. Goy, J.P. Lees, A. Lucotte, M.N. Minard, P. Odier, B. Pietrzyk, et al.

EUROPEAN LABORATORY FOR PARTICLE PHYSICS

CERN/PPE/96-45
21 March 1996

Measurement of hadron and lepton-pair production from e^+e^- annihilation at centre-of-mass energies of 130 and 136 GeV

The ALEPH Collaboration

Abstract

Hadronic and leptonic cross-sections and forward-backward asymmetries are measured using 5.7 pb^{-1} of data taken with the ALEPH detector at LEP at centre-of-mass energies of 130 and 136 GeV. The results agree with Standard Model expectations. The measurement of hadronic cross-sections far away from the Z resonance improves the determination of the interference between photon and Z exchange. Constraints on models with extra Z bosons are presented.

Submitted to Physics Letters B

The ALEPH Collaboration

D. Buskulic, I. De Bonis, D. Decamp, P. Ghez, C. Goy, J.-P. Lees, A. Lucotte, M.-N. Minard, P. Odier, B. Pietrzyk

Laboratoire de Physique des Particules (LAPP), IN^{2}P^3-CNRS, 74019 Annecy-le-Vieux Cedex, France

M.P. Casado, M. Chmeissani, J.M. Crespo, M. Delfino,[12] I. Efthymiopoulos,[20] E. Fernandez, M. Fernandez-Bosman, Ll. Garrido,[15] A. Juste, M. Martinez, S. Orteu, A. Pacheco, C. Padilla, A. Pascual, J.A. Perlas, I. Riu, F. Sanchez, F. Teubert

Institut de Fisica d'Altes Energies, Universitat Autonoma de Barcelona, 08193 Bellaterra (Barcelona), Spain[7]

A. Colaleo, D. Creanza, M. de Palma, G. Gelao, M. Girone, G. Iaselli, G. Maggi,[3] M. Maggi, N. Marinelli, S. Nuzzo, A. Ranieri, G. Raso, F. Ruggieri, G. Selvaggi, L. Silvestris, P. Tempesta, G. Zito

Dipartimento di Fisica, INFN Sezione di Bari, 70126 Bari, Italy

X. Huang, J. Lin, Q. Ouyang, T. Wang, Y. Xie, R. Xu, S. Xue, J. Zhang, L. Zhang, W. Zhao

Institute of High-Energy Physics, Academia Sinica, Beijing, The People's Republic of China[8]

R. Alemany, A.O. Bazarko, P. Bright-Thomas, M. Cattaneo, P. Comas, P. Coyle, H. Drevermann, R.W. Forty, M. Frank, R. Hagelberg, J. Harvey, P. Janot, B. Jost, E. Kneringer, J. Knobloch, I. Lehraus, G. Lutters, E.B. Martin, P. Mato, A. Minten, R. Miquel, Ll.M. Mir,[2] L. Moneta, T. Oest,[1] J.-F. Pusztaszeri, F. Ranjard, P. Rensing,[31] L. Rolandi, D. Schlatter, M. Schmelling,[24] O. Schneider, W. Tejessy, I.R. Tomalin, A. Venturi, H. Wachsmuth, A. Wagner

European Laboratory for Particle Physics (CERN), 1211 Geneva 23, Switzerland

Z. Ajaltouni, A. Barrès, C. Boyer, A. Falvard, P. Gay, C . Guicheney, P. Henrard, J. Jousset, B. Michel, S. Monteil, J-C. Montret, D. Pallin, P. Perret, F. Podlyski, J. Proriol, J.-M. Rossignol

Laboratoire de Physique Corpusculaire, Université Blaise Pascal, IN^{2}P^3-CNRS, Clermont-Ferrand, 63177 Aubière, France

T. Fearnley, J.B. Hansen, J.D. Hansen, J.R. Hansen, P.H. Hansen, B.S. Nilsson, A. Wäänänen

Niels Bohr Institute, 2100 Copenhagen, Denmark[9]

A. Kyriakis, C. Markou, E. Simopoulou, I. Siotis, A. Vayaki, K. Zachariadou

Nuclear Research Center Demokritos (NRCD), Athens, Greece

A. Blondel, J.C. Brient, A. Rougé, M. Rumpf, A. Valassi,[6] H. Videau[21]

Laboratoire de Physique Nucléaire et des Hautes Energies, Ecole Polytechnique, IN^{2}P^3-CNRS, 91128 Palaiseau Cedex, France

E. Focardi,[21] G. Parrini

Dipartimento di Fisica, Università di Firenze, INFN Sezione di Firenze, 50125 Firenze, Italy

M. Corden, C. Georgiopoulos, D.E. Jaffe

Supercomputer Computations Research Institute, Florida State University, Tallahassee, FL 32306-4052, USA [13,14]

A. Antonelli, G. Bencivenni, G. Bologna,[4] F. Bossi, P. Campana, G. Capon, D. Casper, V. Chiarella, G. Felici, P. Laurelli, G. Mannocchi,[5] F. Murtas, G.P. Murtas, L. Passalacqua, M. Pepe-Altarelli

Laboratori Nazionali dell'INFN (LNF-INFN), 00044 Frascati, Italy

L. Curtis, S.J. Dorris, A.W. Halley, I.G. Knowles, J.G. Lynch, V. O'Shea, C. Raine, P. Reeves, J.M. Scarr, K. Smith, A.S. Thompson, F. Thomson, S. Thorn, R.M. Turnbull

Department of Physics and Astronomy, University of Glasgow, Glasgow G12 8QQ,United Kingdom[10]

U. Becker, C. Geweniger, G. Graefe, P. Hanke, G. Hansper, V. Hepp, E.E. Kluge, A. Putzer, B. Rensch, M. Schmidt, J. Sommer, H. Stenzel, K. Tittel, S. Werner, M. Wunsch

Institut für Hochenergiephysik, Universität Heidelberg, 69120 Heidelberg, Fed. Rep. of Germany[16]

D. Abbaneo, R. Beuselinck, D.M. Binnie, W. Cameron, P.J. Dornan, A. Moutoussi, J. Nash, J.K. Sedgbeer, A.M. Stacey, M.D. Williams

Department of Physics, Imperial College, London SW7 2BZ, United Kingdom[10]

G. Dissertori, P. Girtler, D. Kuhn, G. Rudolph

Institut für Experimentalphysik, Universität Innsbruck, 6020 Innsbruck, Austria[18]

A.P. Betteridge, C.K. Bowdery, P. Colrain, G. Crawford, A.J. Finch, F. Foster, G. Hughes, T. Sloan, E.P. Whelan, M.I. Williams

Department of Physics, University of Lancaster, Lancaster LA1 4YB, United Kingdom[10]

A. Galla, A.M. Greene, C. Hoffmann, K. Kleinknecht, G. Quast, B. Renk, E. Rohne, H.-G. Sander, P. van Gemmeren C. Zeitnitz

Institut für Physik, Universität Mainz, 55099 Mainz, Fed. Rep. of Germany[16]

J.J. Aubert,[21] A.M. Bencheikh, C. Benchouk, A. Bonissent,[21] G. Bujosa, D. Calvet, J. Carr, C. Diaconu, N. Konstantinidis, P. Payre, D. Rousseau, M. Talby, A. Sadouki, M. Thulasidas, A. Tilquin, K. Trabelsi

Centre de Physique des Particules, Faculté des Sciences de Luminy, IN^{2}P^3-CNRS, 13288 Marseille, France

M. Aleppo, F. Ragusa[21]

Dipartimento di Fisica, Universitá di Milano e INFN Sezione di Milano, 20133 Milano, Italy.

I. Abt, R. Assmann, C. Bauer, W. Blum, H. Dietl, F. Dydak,[21] G. Ganis, C. Gotzhein, K. Jakobs, H. Kroha, G. Lütjens, G. Lutz, W. Männer, H.-G. Moser, R. Richter, A. Rosado-Schlosser, S. Schael, R. Settles, H. Seywerd, R. St. Denis, W. Wiedenmann, G. Wolf

Max-Planck-Institut für Physik, Werner-Heisenberg-Institut, 80805 München, Fed. Rep. of Germany[16]

J. Boucrot, O. Callot, A. Cordier, M. Davier, L. Duflot, J.-F. Grivaz, Ph. Heusse, A. Höcker, M. Jacquet, D.W. Kim,[19] F. Le Diberder, J. Lefrançois, A.-M. Lutz, I. Nikolic, H.J. Park,[19] I.C. Park,[19] M.-H. Schune, S. Simion, J.-J. Veillet, I. Videau, D. Zerwas

Laboratoire de l'Accélérateur Linéaire, Université de Paris-Sud, IN^{2}P^3-CNRS, 91405 Orsay Cedex, France

P. Azzurri, G. Bagliesi, G. Batignani, S. Bettarini, C. Bozzi, G. Calderini, M. Carpinelli, M.A. Ciocci, V. Ciulli, R. Dell'Orso, R. Fantechi, I. Ferrante, A. Giassi, A. Gregorio, F. Ligabue, A. Lusiani, P.S. Marrocchesi, A. Messineo, F. Palla, G. Rizzo, G. Sanguinetti, A. Sciabà, P. Spagnolo, J. Steinberger, R. Tenchini, G. Tonelli,[26] C. Vannini, P.G. Verdini, J. Walsh

Dipartimento di Fisica dell'Università, INFN Sezione di Pisa, e Scuola Normale Superiore, 56010 Pisa, Italy

G.A. Blair, L.M. Bryant, F. Cerutti, J.T. Chambers, Y. Gao, M.G. Green, T. Medcalf, P. Perrodo, J.A. Strong, J.H. von Wimmersperg-Toeller

Department of Physics, Royal Holloway & Bedford New College, University of London, Surrey TW20 OEX, United Kingdom[10]

D.R. Botterill, R.W. Clifft, T.R. Edgecock, S. Haywood, P. Maley, P.R. Norton, J.C. Thompson, A.E. Wright

Particle Physics Dept., Rutherford Appleton Laboratory, Chilton, Didcot, Oxon OX11 OQX, United Kingdom[10]

B. Bloch-Devaux, P. Colas, S. Emery, W. Kozanecki, E. Lançon, M.C. Lemaire, E. Locci, B. Marx, P. Perez, J. Rander, J.-F. Renardy, A. Roussarie, J.-P. Schuller, J. Schwindling, A. Trabelsi, B. Vallage

CEA, DAPNIA/Service de Physique des Particules, CE-Saclay, 91191 Gif-sur-Yvette Cedex, France[17]

S.N. Black, J.H. Dann, R.P. Johnson, H.Y. Kim, A.M. Litke, M.A. McNeil, G. Taylor

Institute for Particle Physics, University of California at Santa Cruz, Santa Cruz, CA 95064, USA[22]

C.N. Booth, R. Boswell, C.A.J. Brew, S. Cartwright, F. Combley, A. Koksal, M. Letho, W.M. Newton, J. Reeve, L.F. Thompson

Department of Physics, University of Sheffield, Sheffield S3 7RH, United Kingdom[10]

A. Böhrer, S. Brandt, V. Büscher, G. Cowan, C. Grupen, P. Saraiva, L. Smolik, F. Stephan,

Fachbereich Physik, Universität Siegen, 57068 Siegen, Fed. Rep. of Germany[16]

M. Apollonio, L. Bosisio, R. Della Marina, G. Giannini, B. Gobbo, G. Musolino

Dipartimento di Fisica, Università di Trieste e INFN Sezione di Trieste, 34127 Trieste, Italy

J. Putz, J. Rothberg, S. Wasserbaech, R.W. Williams

Experimental Elementary Particle Physics, University of Washington, WA 98195 Seattle, U.S.A.

S.R. Armstrong, L. Bellantoni,[23] P. Elmer, Z. Feng,[28] D.P.S. Ferguson, Y.S. Gao,[29] S. González, J. Grahl, T.C. Greening, J.L. Harton,[27] O.J. Hayes, H. Hu, P.A. McNamara III, J.M. Nachtman, W. Orejudos, Y.B. Pan, Y. Saadi, M. Schmitt, I.J. Scott, V. Sharma,[25] A.M. Walsh,[30] Sau Lan Wu, X. Wu, J.M. Yamartino, M. Zheng, G. Zobernig

Department of Physics, University of Wisconsin, Madison, WI 53706, USA[11]

---

[1] Now at DESY, Hamburg, Germany.
[2] Supported by Dirección General de Investigación Científica y Técnica, Spain.
[3] Now at Dipartimento di Fisica, Università di Lecce, 73100 Lecce, Italy.
[4] Also Istituto di Fisica Generale, Università di Torino, Torino, Italy.
[5] Also Istituto di Cosmo-Geofisica del C.N.R., Torino, Italy.
[6] Supported by the Commission of the European Communities, contract ERBCHBICT941234.
[7] Supported by CICYT, Spain.
[8] Supported by the National Science Foundation of China.
[9] Supported by the Danish Natural Science Research Council.
[10] Supported by the UK Particle Physics and Astronomy Research Council.
[11] Supported by the US Department of Energy, grant DE-FG0295-ER40896.
[12] Also at Supercomputations Research Institute, Florida State University, Tallahassee, U.S.A.
[13] Supported by the US Department of Energy, contract DE-FG05-92ER40742.
[14] Supported by the US Department of Energy, contract DE-FC05-85ER250000.
[15] Permanent address: Universitat de Barcelona, 08208 Barcelona, Spain.
[16] Supported by the Bundesministerium für Forschung und Technologie, Fed. Rep. of Germany.
[17] Supported by the Direction des Sciences de la Matière, C.E.A.
[18] Supported by Fonds zur Förderung der wissenschaftlichen Forschung, Austria.
[19] Permanent address: Kangnung National University, Kangnung, Korea.
[20] Now at CERN, 1211 Geneva 23, Switzerland.
[21] Also at CERN, 1211 Geneva 23, Switzerland.
[22] Supported by the US Department of Energy, grant DE-FG03-92ER40689.
[23] Now at Fermi National Accelerator Laboratory, Batavia, IL 60510, USA.
[24] Now at Max-Plank-Institüt für Kernphysik, Heidelberg, Germany.
[25] Now at University of California at San Diego, La Jolla, CA 92093, USA.
[26] Also at Istituto di Matematica e Fisica, Università di Sassari, Sassari, Italy.
[27] Now at Colorado State University, Fort Collins, CO 80523, USA.
[28] Now at The Johns Hopkins University, Baltimore, MD 21218, U.S.A.
[29] Now at Harvard University, Cambridge, MA 02138, U.S.A.
[30] Now at Rutgers University, Piscataway, NJ 08855-0849, U.S.A.
[31] Now at Dragon Systems, Newton, MA 02160, U.S.A.

1 Introduction

The successful increase of the LEP centre-of-mass energy up to 140 GeV at the end of 1995 allows tests of the Standard Model (SM) at energies so far unexplored. In particular, cross-sections and asymmetries are sensitive not only to the neutral current couplings, as they were at the Z peak, but also to the interference between the Z and the photon, and possibly to the interference with new channels, such as extra Z bosons.

This letter presents measurements of cross-sections and forward-backward asymmetries for $e^+e^- \to f\bar{f}(\gamma)$ and the resulting determination of the γ-Z interference term, as well as limits on possible Z′ bosons.

A description of the ALEPH detector can be found in ref. [1], and an account of its performance as well as a description of the standard analysis algorithms in ref. [2]. The experimental conditions at higher energies differ from those encountered so far in the vicinity of the Z peak. The cross-sections of interest, $e^+e^- \to f\bar{f}(\gamma)$ with an invariant mass of the $f\bar{f}$ system at or near to the full centre-of-mass energy, are now more than two orders of magnitude smaller than those at the Z resonance. Substantial backgrounds from $\gamma\gamma$ processes and from the radiative tail of the Z resonance have to be removed using new cuts. Therefore the analysis techniques have been modified with respect to those described in previous ALEPH publications [3, 4]. Similar analyses have been made by other LEP experiments [5].

2 Luminosity measurements

Given the uncertainties concerning background in this new energy domain, it was decided to use the LCAL calorimeter as the primary luminosity monitoring device for these data. The luminosity is measured following the analysis procedure previously described in [3, 4, 6]. The SICAL detector, placed in front of LCAL, shadows the LCAL at polar angles below 59 mrad. The LCAL geometrical acceptance is therefore slightly reduced with respect to that described in [6]. The integrated luminosities collected at 130 and 136 GeV are 2877 ± 18 nb^{-1} and 2863 ± 19 nb^{-1}, respectively, where the errors are statistical. About 50 nb^{-1} collected at 140 GeV are not included in the analysis presented here.

The experimental systematic uncertainty on the integrated luminosity is estimated to be $\pm 0.75\%$, dominated by the statistics of the Monte Carlo simulation ($\pm 0.54\%$). The theoretical systematic uncertainty, associated with the Monte Carlo generator BHLUMI [7], has been estimated in [8] to be $\pm 0.25\%$. The combined systematic uncertainty is thus $\pm 0.8\%$. The LCAL luminosity is consistent with the luminosity measured independently with the SICAL detector.

3 Cross-sections and forward-backward asymmetries

For a large number of events, initial state photon radiation (ISR) lowers $\sqrt{s'}$, the invariant mass of the final state particles including possible final state radiation, to values close to the Z mass. By demanding that $\sqrt{s'}$ approaches the nominal centre-of-mass energy $\sqrt{s}$, thus allowing for only a few GeV of ISR, cross-sections and asymmetries become more

sensitive to the relevant electroweak effects at high energy. Therefore results are given for two conditions:

- exclusive interaction, i.e. excluding the radiative return to the Z resonance by applying a tight s' cut ($\sqrt{s'/s} > 0.9$).
- inclusive interaction, i.e. including hard ISR with a loose s' cut (i.e. $\sqrt{s'/s} > 0.1$ for $\mathrm{q\overline{q}}$ and $\sqrt{s'} > 2m_\ell$ for leptons, where m_ℓ is the mass of lepton ℓ).

The experimental cuts, however, differ from these definitions, as will be explained in the following. The selection efficiency is therefore calculated by applying the experimental cuts to fully reconstructed simulated events generated within the above defining cuts.

In the event generators used, PYTHIA [9] for $\mathrm{q\overline{q}}$, KORALZ [10] for $\tau^+\tau^-$ and $\mu^+\mu^-$ and UNIBAB [11] for $\mathrm{e^+e^-}$, interference between initial and final state radiation is not considered and the above cross-section definitions are straightforward. This interference was studied separately using ZFITTER [12] and BHM [13], found to be less than 10% of the experimental errors of this analysis, and therefore neglected. Final state radiation as well as transverse momentum of the ISR photons are simulated with a precision adequate for this analysis by all the generators used.

Hadronic and leptonic final states are analysed at centre-of-mass energies of 130.2 GeV and 136.2 GeV. The uncertainty on these energies is ± 60 MeV [14], which has a negligible impact on the physics interpretation of the results.

3.1 Leptonic event selection

The lepton pair selections proceed as described in [3, 4], with some differences which are outlined below.

For all lepton species, the acollinearity cut is removed. An approximate value of s', s'_{m}, is obtained from the following equation:

$$s'_{\mathrm{m}} = s \, \frac{\sin\theta_+ + \sin\theta_- - |\sin(\theta_+ + \theta_-)|}{\sin\theta_+ + \sin\theta_- + |\sin(\theta_+ + \theta_-)|}, \qquad (1)$$

where θ_+ and θ_- are the measured angles of the final state ℓ^+ and ℓ^- with respect to the direction of the incoming $\mathrm{e^-}$ beam. This expression would be exact, in absence of experimental errors, if only one ISR photon were emitted along the beam line. For the tau leptons, θ_+ and θ_- are approximated by the directions of the jets reconstructed from the visible particles of the tau decay. In order to determine the exclusive cross-sections, events with $\sqrt{s'_{\mathrm{m}}/s} > 0.9$ are selected.

Leptons are accepted in the angular range $|\cos\theta^*| < 0.9$, where θ^* is the estimated scattering angle between the incoming $\mathrm{e^-}$ and the outgoing ℓ^- in the $\ell^+\ell^-$ rest frame, defined as $\cos\theta^* = \cos\frac{1}{2}(\theta_- + \pi - \theta_+)/\cos\frac{1}{2}(\theta_- - \pi + \theta_+)$.

For the $\mathrm{e^+e^-}$ channel, which is dominated by the t-channel photon exchange, only the exclusive selection is made. Contrary to what was done at the Z, cross-sections and asymmetries are measured without subtracting the t-channel contribution.

In the $\mu^+\mu^-$ selection the kinematic cuts described in [3, 4] have been replaced by cuts on s'_{m} and on the invariant mass of the two most energetic tracks. It is required that the

Table 1: Efficiencies and background corrections for the different channels at centre-of-mass energy of 130 and 136 GeV with loose and tight s' cut. The efficiency gives the fraction of events above the chosen s' cut passing the experimental selection. In the e^+e^- channel the efficiency is calculated within the angular acceptance $-0.9 < \cos\theta^* < 0.9$.

	efficiency (%)	background (%)
	130 GeV	
$q\bar{q}$	92.6 ± 0.7	1.5 ± 0.5
$\mu^+\mu^-$	72.7 ± 0.5	2.6 ± 1.4
$\tau^+\tau^-$	54 ± 1	9 ± 2
	136 GeV	
$q\bar{q}$	94.3 ± 0.7	2.1 ± 0.7
$\mu^+\mu^-$	70.9 ± 0.5	2.6 ± 1.4
$\tau^+\tau^-$	51 ± 1	11 ± 2
	130 GeV, $\sqrt{s'/s} > 0.9$	
$q\bar{q}$	82.1 ± 1.5	13.3 ± 2.7
e^+e^-	97.3 ± 0.2	negl.
$\mu^+\mu^-$	75.5 ± 0.7	1.1 ± 0.2
$\tau^+\tau^-$	63 ± 2	16 ± 2
	136 GeV, $\sqrt{s'/s} > 0.9$	
$q\bar{q}$	88.2 ± 1.5	12.3 ± 2.7
e^+e^-	97.2 ± 0.2	negl.
$\mu^+\mu^-$	75.5 ± 0.7	1.7 ± 0.2
$\tau^+\tau^-$	60 ± 2	15 ± 2

invariant mass be greater than 80 GeV for the inclusive selection and 110 GeV for the exclusive one. The residual background quoted in table 1 originates from $\gamma\gamma$ events in the inclusive analysis, and from events with hard ISR photons in the exclusive analysis.

The $\tau^+\tau^-$ selection rejects identified $\mu^+\mu^-$ and e^+e^- pairs to reduce the background from $\gamma\gamma \to \mu^+\mu^-$, e^+e^- and from Bhabha events. Low polar angle events ($|\cos\theta^*| > 0.75$) with only one identified electron are removed if their total visible energy exceeds $0.9\sqrt{s}$. The $\gamma\gamma$ background is further reduced by requiring that the quantity $\sqrt{P_{\mathrm{ch},1}^2 + P_{\mathrm{ch},2}^2}$ be in excess of $0.1\sqrt{s}$, $P_{\mathrm{ch,i}}$ being the vector sum of the momenta of all charged tracks in hemisphere i. These cuts reduce the total background to a level of 10% in the case of the inclusive selection (dominated by $\gamma\gamma \to \tau^+\tau^-$, $\mu^+\mu^-$), and to about 15% for the exclusive selection (dominated by $\tau^+\tau^-$ events with hard ISR photons).

Table 2: Cross-sections with statistical and systematic errors, respectively, for different channels at the centre-of-mass energy of 130 and 136 GeV with loose and tight s' cuts. Cross-sections are extrapolated to the full angular range, except for the e^+e^- where they are given only for $|\cos\theta^*| < 0.9$. The second column gives the number of events after experimental cuts and before efficiency and background corrections. The last column shows the SM predictions.

	events	σ (pb)	SM predictions (pb)
		130 GeV	
$q\bar{q}$	889	$327.7 \pm 11.0 \pm 2.8$	336.3
$\mu^+\mu^-$	49	$22.9 \pm 3.4 \pm 0.4$	24.8
$\tau^+\tau^-$	47	$28.2 \pm 4.4 \pm 1.0$	22.7
		136 GeV	
$q\bar{q}$	755	$272.8 \pm 9.9 \pm 2.7$	279.9
$\mu^+\mu^-$	43	$20.6 \pm 3.2 \pm 0.3$	21.4
$\tau^+\tau^-$	38	$22.4 \pm 4.1 \pm 0.9$	19.5
		130 GeV, $\sqrt{s'/s} > 0.9$	
$q\bar{q}$	203	$74.2 \pm 5.2 \pm 3.3$	76.9
e^+e^-	614	$219.4 \pm 9.0 \pm 1.0$	212.4
$\mu^+\mu^-$	23	$9.6 \pm 1.9 \pm 0.1$	8.0
$\tau^+\tau^-$	26	$11.8 \pm 2.3 \pm 0.4$	8.0
		136 GeV, $\sqrt{s'/s} > 0.9$	
$q\bar{q}$	166	$57.4 \pm 4.5 \pm 1.8$	62.5
e^+e^-	551	$197.0 \pm 8.6 \pm 1.0$	194.2
$\mu^+\mu^-$	17	$7.1 \pm 1.7 \pm 0.1$	6.9
$\tau^+\tau^-$	11	$5.8 \pm 1.7 \pm 0.2$	6.9

3.2 Hadronic event selection

Hadronic events are first selected by requiring at least five good charged tracks. Good tracks are reconstructed from at least four hits in the Time Projection Chamber and originate from within a cylinder of 2 cm radius and 20 cm length, coaxial with the beam axis and centered on the nominal interaction point. The polar angles θ of these tracks, measured with respect to the beam axis, should be such that $|\cos\theta| < 0.95$. The visible invariant mass $m_{\rm vis}$ is then calculated from all charged and neutral objects [2] with a polar angle greater than 190 mrad with respect to the beam axis. The resulting distribution (fig. 1a) shows a large background from $\gamma\gamma$ interactions at low mass values; therefore only events with mass above 50 GeV are selected. The remaining event sample consists of three different components: radiative events with hard ISR photons escaping detection,

for which $m_{\rm vis}$ is peaked at the Z mass; radiative events with hard ISR photons detected in the apparatus; exclusive interactions with no hard ISR. For these last two components $m_{\rm vis}$ is close to the centre-of-mass energy. To separate them, energetic isolated photons are tagged by reconstructing jets with the JADE algorithm with a $y_{\rm cut}$ of 0.008 and requiring that the jet electromagnetic component (defined as the fraction of the jet energy carried by photon and electron candidates) be larger than 95% (fig. 1b). The energy spectrum of the jets with high electromagnetic fraction matches the Monte Carlo expectation for ISR photons (fig. 1c). As expected, the energy spectrum of these photons is peaked at $(s - m_{\rm Z}^2)/2\sqrt{s}$. The visible invariant mass is then recalculated without these photon candidates and is shown in fig. 1d.

For the exclusive interaction cross-section, the measurement of $s'_{\rm m}$ is performed as follows. All events are forced into a two-jet topology, after removal of the photon candidates, by adjusting the $y_{\rm cut}$ parameter. In this case, θ_+ and θ_- of eq. 1 are the angles of the two jets with respect to *i*) the detected photon direction, *ii*) the beam axis, if no photon is detected. Figure 2a shows the $\sqrt{s'_{\rm m}/s}$ distributions for data and Monte Carlo samples at a centre-of-mass energy of 136 GeV. For inclusive cross-section measurements, a cut of $\sqrt{s'_{\rm m}/s} > 0.45$ is applied, reducing the residual $\gamma\gamma$ background by a factor of two. The visible invariant mass distributions for data reconstructed in the regions $\sqrt{s'_{\rm m}/s} > 0.45$ and $\sqrt{s'_{\rm m}/s} > 0.9$ are shown in figure 2b.

Monte Carlo simulations are used to calculate the efficiencies and background contaminations shown in table 1. The backgrounds for the inclusive selections are dominated by the $\gamma\gamma$ processes, to which an uncertainty of 30% is attributed after comparing the simulated events with data reconstructed at low invariant mass. Therefore these errors are fully correlated between the two centre-of-mass energies. Beam-gas and cosmic ray backgrounds are found to be negligible in the present selection. For the exclusive selections, events where both incoming electron and positron radiate represent the main remaining source of background. This background is monitored by comparing the visible invariant mass spectra of events with $\sqrt{s'_{\rm m}/s} > 0.9$ both in data and Monte Carlo samples in the region of $m_{\rm vis} < 105$ GeV. The statistical error on the number of events in this region in each data sample is used to estimate the background uncertainty. Therefore these errors for the two centre-of-mass energies are uncorrelated.

3.3 Results

Efficiency and background contamination for the different channels are summarized in table 1, and the corresponding cross-sections in table 2. Cross-sections are extrapolated to the full angular range, except for the $\rm e^+e^-$ where they are given only for $|\cos\theta^*| < 0.9$. The systematic errors include both efficiency and background subtraction errors. The luminosity systematic error of 0.8%, common to all channels, is not included in the numbers quoted in the table. The measured $\rm q\overline{q}$, $\rm e^+e^-$, $\mu^+\mu^-$ and $\tau^+\tau^-$ cross-sections are shown in fig. 3 as functions of the centre-of-mass energy. Agreement with the SM prediction is observed.

Lepton forward-backward asymmetries are given in table 3. All lepton asymmetries are calculated by counting events in the forward and backward hemispheres within the angular range $|\cos\theta^*| < 0.9$. The $\rm e^+e^-$ forward-backward asymmetry is about 95% in the

Table 3: Results on lepton forward-backward asymmetries with statistical errors for loose and tight s' cuts. The last column shows the SM predictions.

	A_{FB}	SM predictions
	130 GeV	
$\mu^+\mu^-$	$0.39^{+0.14}_{-0.16}$	0.25
$\tau^+\tau^-$	$0.60^{+0.13}_{-0.16}$	0.27
	136 GeV	
$\mu^+\mu^-$	$0.23^{+0.16}_{-0.17}$	0.24
$\tau^+\tau^-$	$0.30^{+0.18}_{-0.21}$	0.27
	130 GeV, $\sqrt{s'/s} > 0.9$	
e^+e^-	$0.93^{+0.01}_{-0.02}$	0.95
$\mu^+\mu^-$	$0.65^{+0.16}_{-0.23}$	0.66
$\tau^+\tau^-$	$0.91^{+0.08}_{-0.20}$	0.66
	136 GeV, $\sqrt{s'/s} > 0.9$	
e^+e^-	$0.94^{+0.01}_{-0.02}$	0.95
$\mu^+\mu^-$	$0.53^{+0.22}_{-0.29}$	0.64
$\tau^+\tau^-$	$0.70^{+0.18}_{-0.42}$	0.64

chosen angular acceptance due to the large contribution of t-channel photon exchange at these high energies. Errors are statistical only. No systematic errors are given since they are negligible compared to the statistical errors. Agreement with the SM prediction is also observed.

For hadronic events, the average difference of charge between the forward and backward hemispheres, $Q_{\rm FB}$, is obtained from the momentum-weighted charge of particles, as described in reference [15]. The hemispheres are defined by the thrust axis in events selected with $\sqrt{s'_{\rm m}/s} > 0.9$ and $|\cos\theta_{\rm thr}| < \cos\theta^{\rm max}_{\rm thr}$, where $\cos\theta^{\rm max}_{\rm thr} = 0.9$.

In contrast to the Z resonance, where this asymmetry is dominated by the contribution of the d-type quarks, at these high energies $Q_{\rm FB}$ is dominated by the contribution of u-type quarks. Consequently, the optimal sensitivity is obtained for a different value of the momentum weighting exponent κ (i.e. $\kappa = 0.3$ while $\kappa = 1.0$ is used at $\sqrt{s} \sim m_{\rm Z}$). For this choice of κ the measured value of $\langle Q_{\rm FB}\rangle$ is $3.6 \pm 1.8\%$, where the events from centre-of-mass energies of 130 and 136 GeV are combined.

The theoretical expectation of this observable is given by

$$\langle Q_{\rm FB}\rangle = \langle Q_{\rm F} - Q_{\rm B}\rangle = \sum_q \delta_{\rm q} \frac{\sigma_{\rm q}}{\sigma_{\rm had}} A^{\rm q}_{\rm FB} \frac{4\cos\theta^{\rm max}_{\rm thr}}{3 + \cos^2\theta^{\rm max}_{\rm thr}}, \qquad (2)$$

where the summation is made over quark flavours $\rm q = u, d, c, s, b$. The charge separation for each flavour, $\delta_{\rm q}$, describes the average difference in hemisphere charge between the hemisphere containing the primary quark q and that containing the corresponding

antiquark $\bar{q}$. The charge separations are determined from a Monte Carlo sample at $\sqrt{s} = 140$ GeV, with additional corrections obtained from the more precise analysis at the Z resonance [16]. The estimated values for $\kappa = 0.3$ and $\sqrt{s}$=133 GeV are given in table 4. The uncertainties are dominated by Monte Carlo statistics. The expected value for Q_{FB} using these charge separations and the SM cross-sections and asymmetries is $2.5 \pm 0.5\%$, in good agreement with the measurement.

Table 4: Charge separations for each flavour at $\sqrt{s} = 133$ GeV and $\kappa = 0.3$, as determined from simulation.

δ_{u}	δ_{d}	δ_{c}	δ_{s}	δ_{b}
0.16 ± 0.02	-0.09 ± 0.02	0.19 ± 0.02	-0.13 ± 0.03	-0.10 ± 0.01

4 Determination of the γ-Z interference in the hadronic channel

The data taken at 130 and 136 GeV are fitted together with those taken at the centre-of-mass energies close to the Z peak in order to determine the parameters that quantify the γ-Z interference contribution.

The total hadronic cross-section (after deconvolution of the ISR) can be expressed in the S-Matrix formalism [17] as

$$\sigma^0_{\mathrm{h}}(s) = \frac{4}{3}\pi\alpha^2 \left(\frac{\mathrm{g}^{\mathrm{tot}}_{\mathrm{had}}}{s} + \frac{s\,\mathrm{r}^{\mathrm{tot}}_{\mathrm{had}} + (\mathrm{s} - \overline{\mathrm{m}}^2_{\mathrm{Z}})\mathrm{j}^{\mathrm{tot}}_{\mathrm{had}}}{(s - \overline{m}^2_{\mathrm{Z}})^2 + \overline{m}^2_{\mathrm{Z}}\overline{\Gamma}_{\mathrm{Z}}{}^2} \right). \tag{3}$$

The parameters $\overline{m}_{\mathrm{Z}}$ and $\overline{\Gamma}_{\mathrm{Z}}$ are related to the usual definitions of the Z mass and width through the transformations $m_{\mathrm{Z}} = \overline{m}_{\mathrm{Z}} + 34\,\mathrm{MeV}$ and $\Gamma_{\mathrm{Z}} = \overline{\Gamma}_{\mathrm{Z}} + 0.9\,\mathrm{MeV}$. The terms $\mathrm{g}^{\mathrm{tot}}_{\mathrm{had}}$, $\mathrm{r}^{\mathrm{tot}}_{\mathrm{had}}$ and $\mathrm{j}^{\mathrm{tot}}_{\mathrm{had}}$ express the size of the γ exchange, Z exchange and the γ-Z interference, respectively. The parameters $\mathrm{r}^{\mathrm{tot}}_{\mathrm{had}}$ and $\mathrm{j}^{\mathrm{tot}}_{\mathrm{had}}$ can be interpreted in terms of quark couplings through the approximate relations

$$\mathrm{r}^{\mathrm{tot}}_{\mathrm{had}} \propto \sum_{\mathrm{q=u,d,c,s,b}} (\mathrm{g}^2_{\mathrm{Aq}} + \mathrm{g}^2_{\mathrm{Vq}}) \tag{4}$$

$$\mathrm{j}^{\mathrm{tot}}_{\mathrm{had}} \propto \sum_{\mathrm{q=u,d,c,s,b}} \mathrm{Q}_{\mathrm{q}} \times \mathrm{g}_{\mathrm{Vq}} \tag{5}$$

The γ-Z interference contribution is below 0.6% in the centre-of-mass energy region $\sqrt{m_{\mathrm{Z}}} \pm 3$ GeV and it changes sign (equation 3) when crossing the Z pole. Its size parameter, $\mathrm{j}^{\mathrm{tot}}_{\mathrm{had}}$, is fixed to the SM value in the lineshape fits to the data taken near the Z resonance. The error on m_{Z} increases sizeably if $\mathrm{j}^{\mathrm{tot}}_{\mathrm{had}}$ is left free in the fits due to a strong anticorrelation of $\mathrm{j}^{\mathrm{tot}}_{\mathrm{had}}$ and m_{Z}. Inclusion of data far away from the Z resonance, more sensitive to the γ-Z interference contribution, allows a simultaneous fit of $\mathrm{j}^{\mathrm{tot}}_{\mathrm{had}}$ and m_{Z} with higher precision. The results given in this section are obtained by fixing the pure QED contribution $\mathrm{g}^{\mathrm{tot}}_{\mathrm{had}}$ to the SM value.

The expected errors on m_Z and j_{had}^{tot} are shown in fig. 4 as a function of the $\sqrt{s'/s}$ cut. The requirement that $\sqrt{s'/s}$ be greater than 0.9 excludes the radiative return to the Z resonance and improves the precision on j_{had}^{tot} by about 30% with respect to the case without s' cut. Therefore, in the following, the hadronic cross-sections of table 2 with the cut $\sqrt{s'/s} > 0.9$ have been used.

Table 5 shows the fit results for m_Z, Γ_Z, r_{had}^{tot} and j_{had}^{tot} obtained with program [18] modified to fit the S-Matrix parameters. All the published ALEPH data [3, 4] (ALEPH 92), the new high-energy (h.e.) data and the published TOPAZ [19] data are used in the fit. Indeed the TOPAZ Collaboration at TRISTAN (KEK) has recently published a measurement of the hadronic total cross-section at $\sqrt{s} = 57.77$ GeV, $\sigma_h^0 = 143.6 \pm 1.5(stat.) \pm 4.5(syst.)$ pb. This measurement has a strong impact on the determination of j_{had}^{tot}, since the relative contribution of the hadronic γ-Z interference term to the total cross-section is larger at that energy.

Table 5: Results of the fits to the hadronic lineshape using data from: (1) ALEPH 92, (2) ALEPH 92 + h.e., (3) ALEPH 92 + TOPAZ, (4) ALEPH 92 + h.e. + TOPAZ. The SM predictions correspond to $m_Z = 91.188$ GeV, $m_t = 180$ GeV, $m_H = 300$ GeV, $\alpha_s(m_Z^2) = 0.125$ and $1/\alpha(m_Z^2) = 128.896$.

	(1)	(2)	(3)	(4)	SM pred.
m_Z(GeV)	91.205 ± 0.015	91.200 ± 0.012	91.192 ± 0.010	91.193 ± 0.010	-
Γ_Z(GeV)	2.496 ± 0.012	2.498 ± 0.012	2.499 ± 0.012	2.499 ± 0.012	2.498
r_{had}^{tot}	2.975 ± 0.029	2.979 ± 0.029	2.985 ± 0.028	2.984 ± 0.028	2.970
j_{had}^{tot}	-0.82 ± 0.73	-0.47 ± 0.42	0.05 ± 0.25	-0.01 ± 0.20	0.22
χ^2/d.o.f	17.1/23	17.6/25	18.7/24	19.1/26	

The experimental value of j_{had}^{tot}, as obtained by combining the new high energy results with the published ALEPH data and with the TOPAZ hadronic cross-section, is given by

$$j_{had}^{tot} = -0.01 \pm 0.20. \quad (6)$$

This is to be compared with the SM prediction $j_{had}^{tot} = 0.22$. As seen from table 5, the effect of the high-energy data is to reduce the error on j_{had}^{tot} from ± 0.73 to ± 0.42, using ALEPH data alone.

The impact of the data taken far from the Z peak on the determination of j_{had}^{tot} is clearly visible in fig. 5 where the contours of equal probability in the plane m_Z vs j_{had}^{tot} are plotted for the four fits of table 5. The plot also shows how the anticorrelation between m_Z and j_{had}^{tot} (which was -76% for ALEPH 92) is considerably reduced when adding the data taken at 130-136 GeV (-56%), and even more after adding the TOPAZ measurement (-31%).

5 Limits on extra Z bosons

As an example of the potential of a precise measurement of the energy dependence of the total hadronic cross-section in testing possible departures from the SM, a search for

extra Z bosons is presented here for three E_6-based models [20]. After specifying the model (and without any assumption on the structure of the Higgs sector), only two free parameters remain: *i*) the mixing angle θ_3 between Z and Z′, *ii*) the mass of the heavier-mass eigenstate, $m_{Z'}$. Data taken at the Z resonance have already put stringent limits on θ_3 (see for example [4, 21]), but they are only weakly sensitive to $m_{Z'}$, while far away from the Z peak the $m_{Z'}$ sensitivity increases.

The program ZEFIT [22] (with the parameter θ_3 fixed to zero) is used to compute the χ^2 of the fit to the ALEPH and TOPAZ hadronic cross-sections as a function of $m_{Z'}$. This allows the following limits on extra Z bosons to be obtained for three particular models

$$\begin{aligned} m_{Z'} &> 196 \text{ GeV} \quad \text{at } 95\% \text{ C.L.} \quad (\chi \text{ model}) \\ m_{Z'} &> 148 \text{ GeV} \quad \text{at } 95\% \text{ C.L.} \quad (\psi \text{ model}) \\ m_{Z'} &> 167 \text{ GeV} \quad \text{at } 95\% \text{ C.L.} \quad (\eta \text{ model}). \end{aligned}$$

These limits do not change significantly if the lepton forward-backward asymmetries are also included. The limits obtained from direct searches [23] are $m_{Z'} > 340, 320$ and 340 GeV at 95% C.L. for the χ, ψ and η models, respectively.

6 Conclusions

The results on hadronic and leptonic cross-sections and forward-backward asymmetries obtained at centre-of-mass energies of 130 and 136 GeV are in good agreement with the SM expectations. An improvement of the accuracy on the hadronic γ-Z interference has been obtained. For the Z mass measurement this implies a reduced dependence on the assumption of the validity of the SM for the γ-Z interference. Due to the limited integrated luminosity, the bounds on new physics from electroweak measurements are not very stringent compared to those obtained from direct searches.

7 Acknowledgements

We wish to thank and congratulate our colleagues from the accelerator divisions for having been so fast and efficient in operating LEP in this new energy regime. We are also grateful to the engineers and technicians in all our institutions for their contribution to the success of ALEPH. Those of us from non-member states thank CERN for its hospitality.

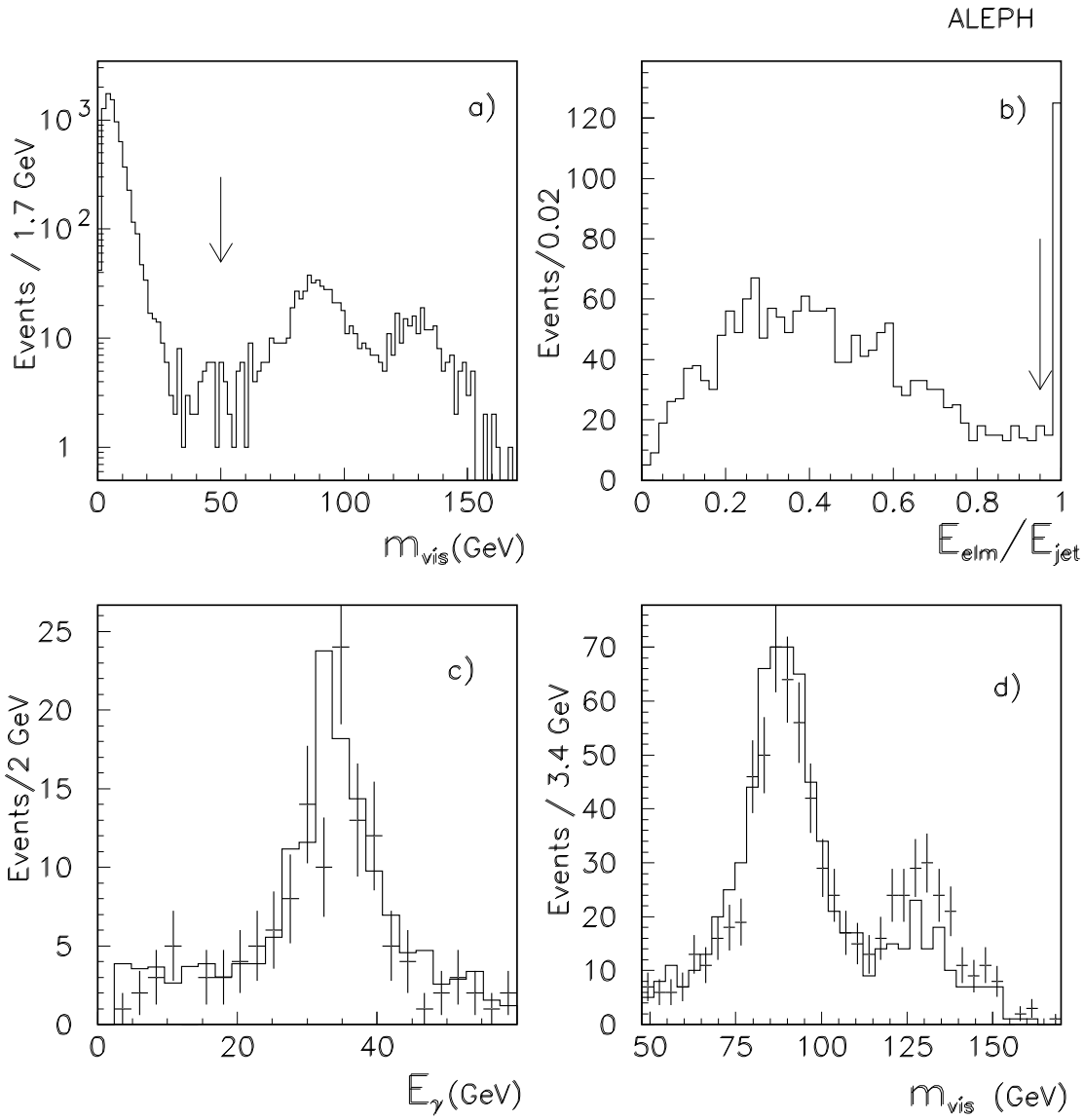

Figure 1: a) Invariant mass of all charged and neutral objects at an angle greater than 190 mrad with respect to the beam axis at centre-of-mass energy of 136 GeV. The arrow shows the 50 GeV cut on the invariant mass. b) Electromagnetic fraction in jet. Jets with an electromagnetic fraction above the cut indicated by the arrow are rejected. c) Energy distribution of jets with high electromagnetic fraction for data (points) and Monte Carlo (histogram). d) Visible invariant mass including (points) and excluding (histogram) jets with high electromagnetic fraction seen in the detector.

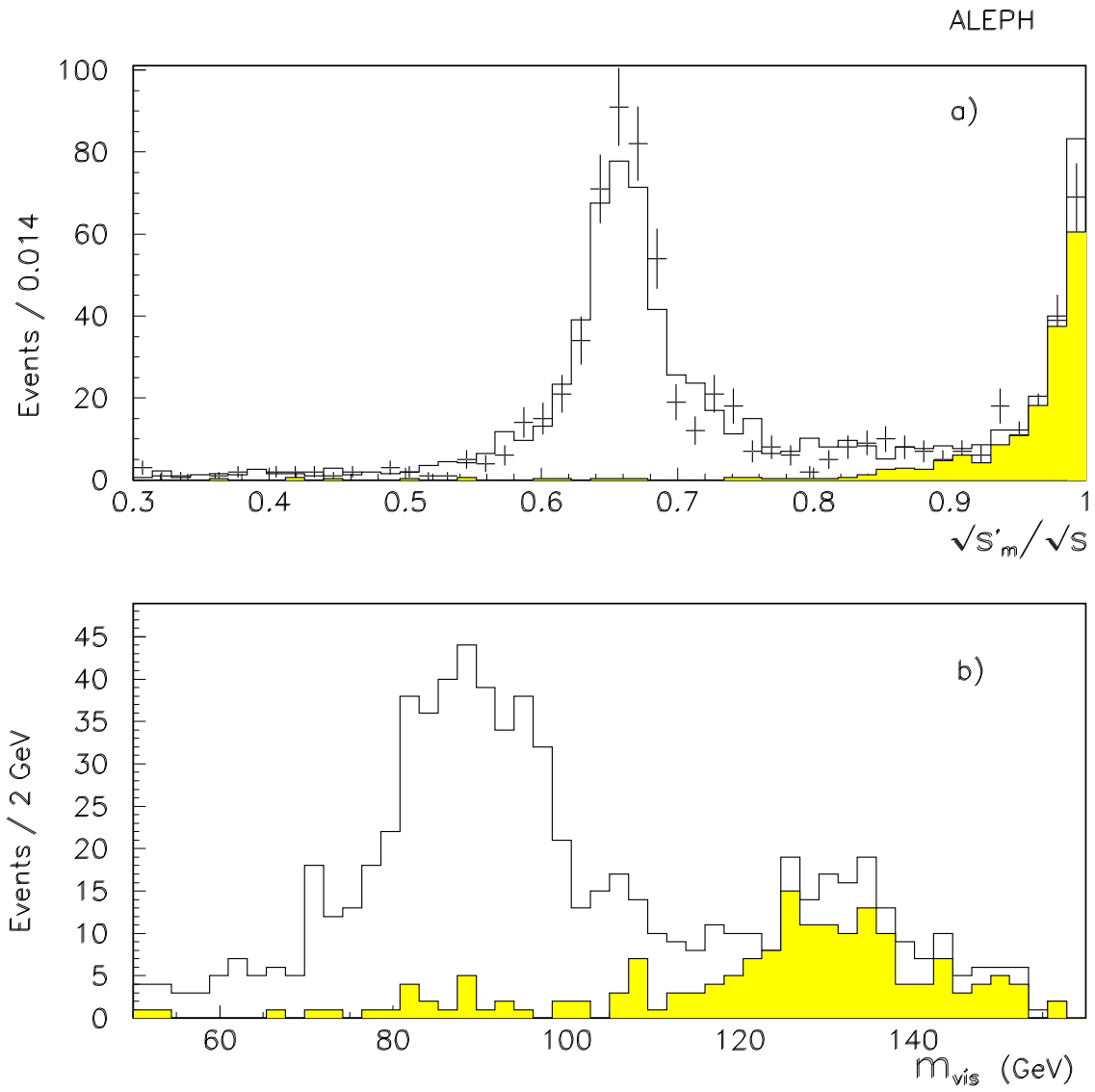

Figure 2: a) Distribution of $\sqrt{s'_{\rm m}/s}$ for data (points) and Monte Carlo (histogram) at centre-of-mass of 136 GeV. The shaded area gives the contribution of Monte Carlo events generated with $\sqrt{s'/s} > 0.9$. b) Distributions of the visible invariant mass without photonic "jets" for data reconstructed in the regions $\sqrt{s'_{\rm m}/s} > 0.45$ and $\sqrt{s'_{\rm m}/s} > 0.9$ (shaded).

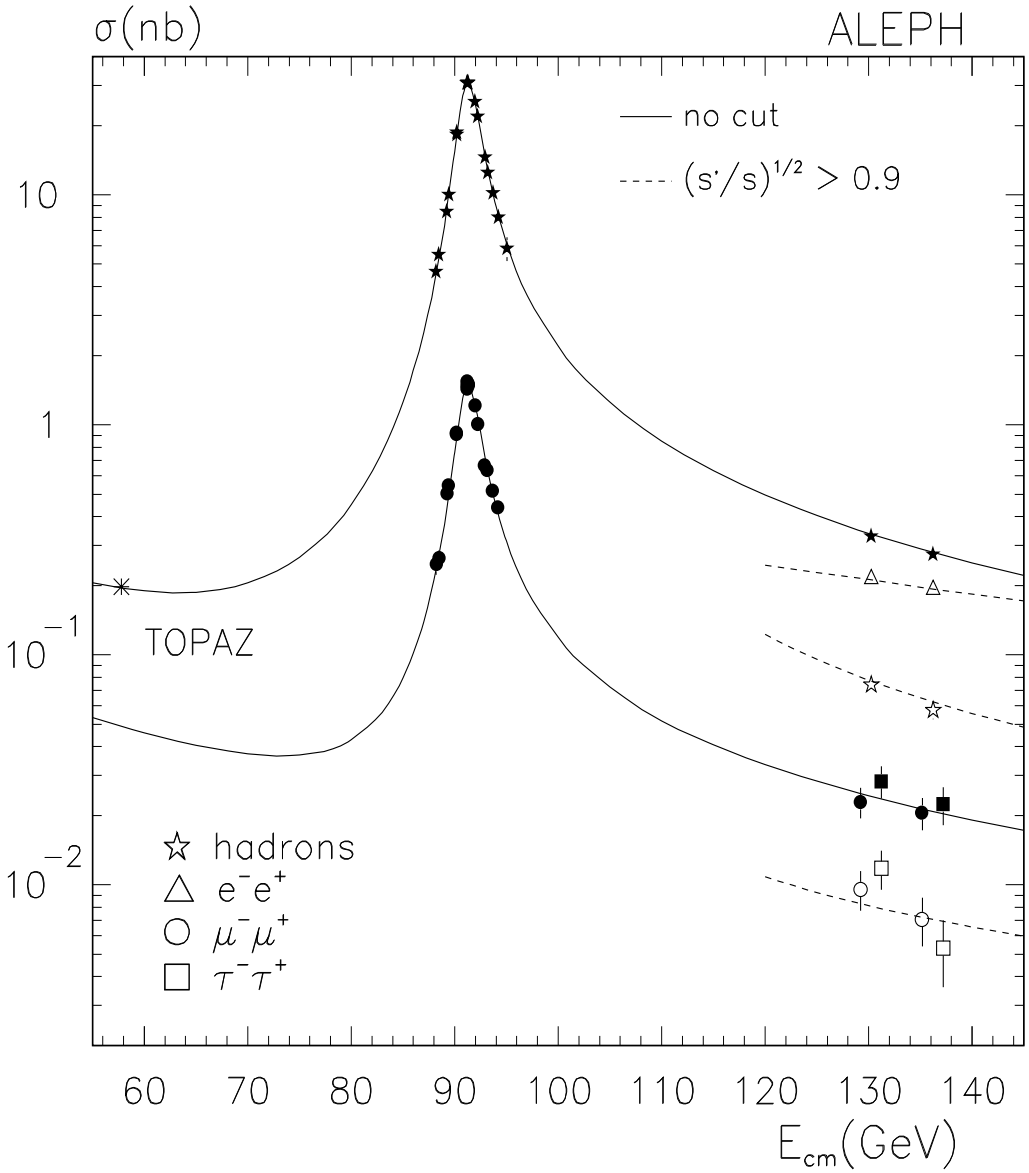

Figure 3: Measured cross-sections and their comparison with the SM predictions. The closed symbols correspond to the inclusive cross-sections, the open ones to the measurements with $\sqrt{s'/s} > 0.9$. For reader's convenience the $\mu^+\mu^-$ and $\tau^+\tau^-$ points have been slightly shifted in energy.

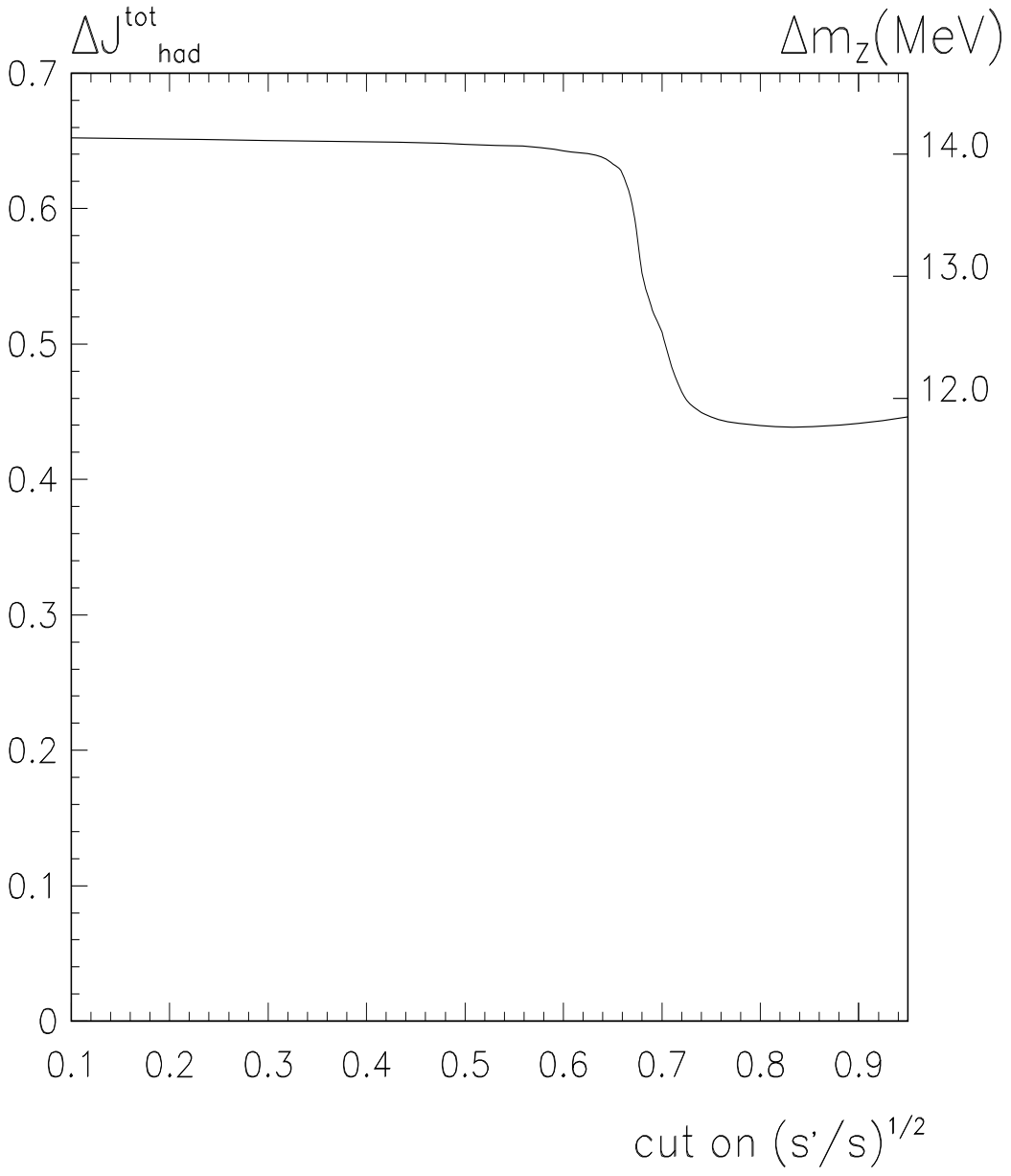

Figure 4: Expected errors on m_{Z} and $\mathrm{j}^{\mathrm{tot}}_{\mathrm{had}}$ as a function of the applied cut on $\sqrt{s'/s}$ calculated for the luminosity, centre-of-mass and experimental efficiencies of the data used for this analysis.

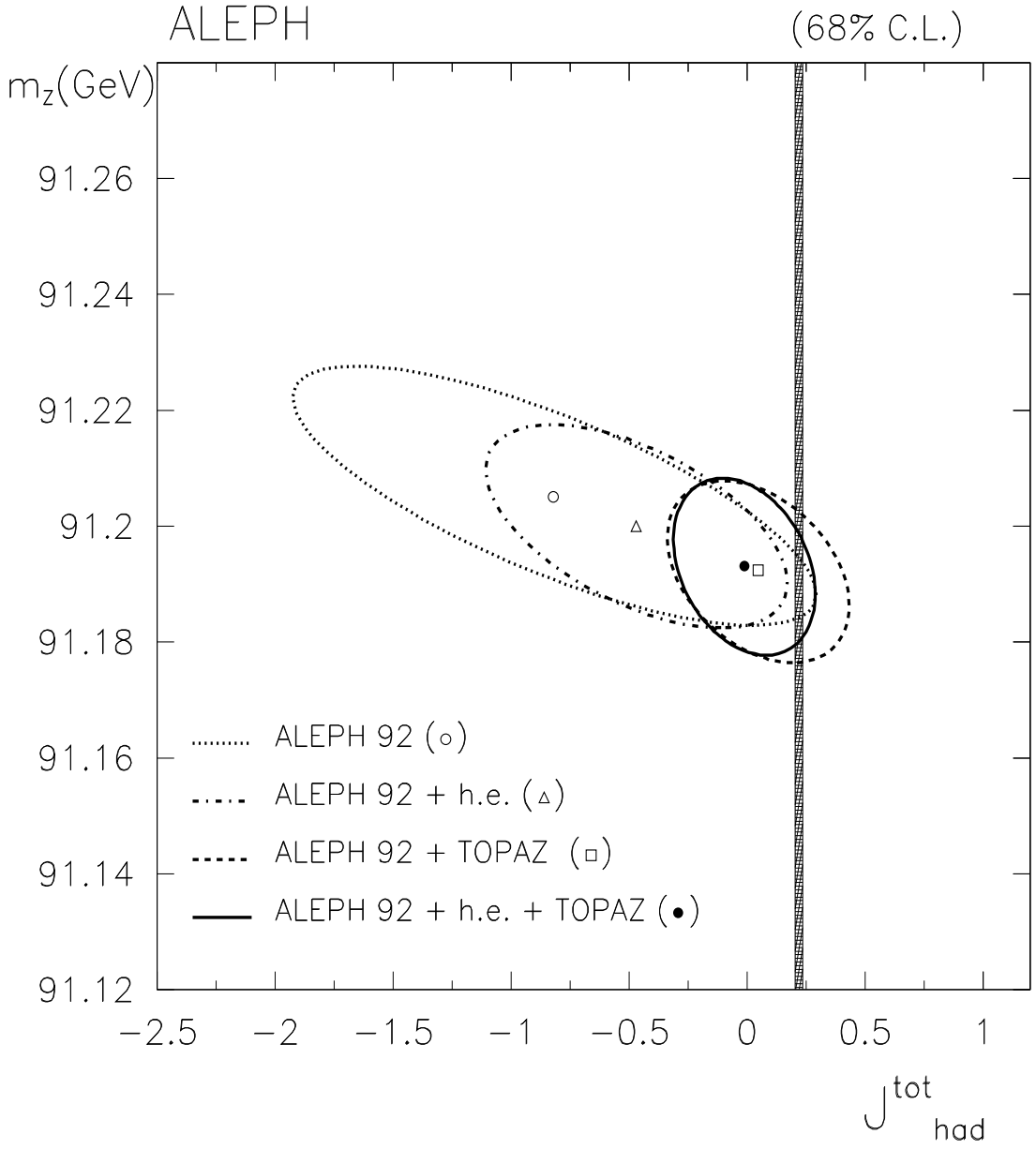

Figure 5: Contours of equal probability containing the 68% probability region in the parameters space. The band correspond to the SM predictions for j^{tot}_{had} when 168 GeV $< m_t <$ 192 GeV and 60 GeV $< m_H <$ 1000 GeV.

References

[1] ALEPH Collaboration, D. Decamp *et al.*, Nucl. Inst. Meth. **A294** (1990) 121.

[2] ALEPH Collaboration, D. Buskulic *et al.*, Nucl. Inst. Meth. **A360** (1995) 481.

[3] ALEPH Collaboration, D. Decamp *et al.*, Z. Phys. **C48** (1990) 365; **C53** (1992) 1; D. Buskulic *et al.*, **C60** (1993) 71.

[4] ALEPH Collaboration, D. Buskulic *et al.*, Z. Phys. **C62** (1994) 539.

[5] L3 Collaboration, M. Acciarri *et al.*, *Measurement of Hadron and Lepton-Pair Production at 130 GeV*$< \sqrt{s} <$ *140 GeV at LEP*, CERN-PPE/95-191 (December 1995), submitted to Phys. Lett. B;
OPAL Collaboration, G. Alexander *et al.*, *Measurement of cross-sections and asymmetries in* e^+e^- *collisions at 130-140 GeV centre-of-mass energy*, CERN-PPE/96-025 (February 1996), submitted to Phys. Lett. B.

[6] ALEPH Collaboration, D. Decamp *et al.*, Z. Phys **C53** (1992) 375.

[7] S. Jadach, E. Richter-Wąs, Z. Wąs and B.F.L. Ward, Phys. Lett. **B268** (1991) 253; Comput. Phys. Comm. **70** (1992) 305. **B268** (1991) 253;

[8] S. Jadach *et al.*, 'Event Generators for Bhabha Scattering', in *Physics at LEP 2*, eds. G. Altarelli, T. Sjöstrand and F. Zwirner (CERN 96-01, Geneva, 1996).

[9] T. Sjöstrand, Comput. Phys. Comm. **82** (1994) 74.

[10] S. Jadach and Z. Wąs, Comput. Phys. Comm. **36** (1985) 191; Monte Carlo Group in *Z Physics at LEP 1*, eds. G. Altarelli, R. Kleiss and C. Verzegnassi (CERN 89-08, Geneva, 1989) Vol. III; S. Jadach, B.F.L. Ward and Z. Wąs, Comput. Phys. Comm. **66** (1991) 276.

[11] H. Anlauf *et al.*, Comput. Phys. Comm. **79** (1994) 466.

[12] D. Bardin *et al.*, Z. Phys. **C44** (1989) 493; Comput. Phys. Comm. **59** (1990) 303; Nucl. Phys. **B351** (1991) 1; Phys. Lett. **B255** (1991) 290 and CERN-TH 6443/92 (May 1992).

[13] G. Burgers, W. Hollik and M. Martinez, FORTRAN program based on *Z Physics at LEP 1*, eds. G. Altarelli, R. Kleiss and C. Verzegnassi (CERN 89-08, Geneva, 1989) Vol. I;
Reports of the working group on precision calculations for the Z resonance, eds. D. Bardin, W. Hollik and G. Passarino (CERN 95-03, Geneva, 1995).

[14] The LEP Energy Working Group, private communication.

[15] ALEPH Collaboration, D. Decamp *et al.*, Phys. Lett., **B259** (1991) 377.

[16] ALEPH Collaboration, D. Busculic *et al.*, *Determination of* $sin^2\theta_W^{eff}$ *Using Jet Charge Measurements in Hadronic Z Decays*, CERN-PPE/96-09 (January 1996), submitted to Z. Phys.

[17] R.G. Stuart, Phys. Lett. **B272** (1991) 353;
A. Leike, T. Riemann and J. Rose, Phys. Lett. **B273** (1991) 513;
T. Riemann, Phys. Lett. **B293** (1992) 451.

[18] M. Martinez, L. Garrido, R. Miquel, J.L. Harton and R. Tanaka, Z. Phys. **C49** (1991) 645.

[19] TOPAZ Collaboration, K. Miyabayashi *et al.*, Phys. Lett. **B347** (1995) 171.

[20] R.W. Robinett, Phys. Rev. **D26** (1982) 2388;
R.W. Robinett, J.L. Rosner, Phys. Rev. **D26** (1982) 2396;
F. del Aguila, G. Blair, M. Daniel, G.G. Ross, Nucl. Phys. **B272** (1986) 413;
J.L. Hewett, T.G. Rizzo, J.A. Robinson, Phys. Rev. **D33** (1986) 1476, **D34** (1986) 2179;
D. London, J.L. Rosner, Phys. Rep. **34** (1986) 1530;
P. Binetruy, S. Dawson, T. Hinchliffe, M. Sher, Nucl. Phys. **B273** (1986) 501;
J. Ellis, K. Enqvist, D.V. Nanopoulos, F. Zwirner, Nucl. Phys. **B276** (1986) 14;
G. Belanger, S. Godfrey, Phys. Rev. **D35** (1987) 378.

[21] G. Altarelli *et al.*, Phys. Lett. **B318** (1993) 139.

[22] A. Leike, S. Riemann, T. Riemann, University of Munich preprint LMU-91/06 and FORTRAN program ZEFIT; Phys. Lett. **B291** (1992) 187.

[23] CDF Collaboration, F. Abe *et al.*, Phys. Rev. Lett. **68** (1992) 1463.